

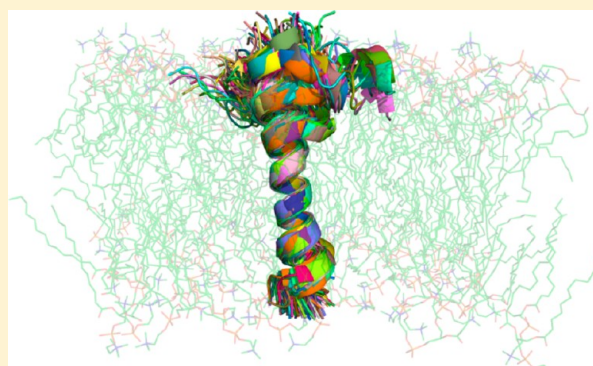
# Structural Determinants for the Membrane Insertion of the Transmembrane Peptide of Hemagglutinin from Influenza Virus

Bruno L. Victor,\* António M. Baptista, and Cláudio M. Soares

Instituto de Tecnologia Química e Biológica, Universidade Nova de Lisboa Avenida da República, EAN Apartado 127, 2781-901 Oeiras, Portugal

## Supporting Information

**ABSTRACT:** Membrane fusion is a process involved in a high range of biological functions, going from viral infections to neurotransmitter release. Fusogenic proteins increase the slow rate of fusion by coupling energetically downhill conformational changes of the protein to the kinetically unfavorable fusion of the membrane lipid bilayers. Hemagglutinin is an example of a fusogenic protein, which promotes the fusion of the membrane of the influenza virus with the membrane of the target cell. The N-terminus of the HA2 subunit of this protein contains a fusion domain described to act as a destabilizer of the target membrane bilayers, leading eventually to a full fusion of the two membranes. On the other hand, the C-terminus of the same subunit contains a helical transmembrane domain which was initially described to act as the anchor of the protein to the membrane of the virus. However, in recent years the study of this peptide segment has been gaining more attention since it has also been described to be involved in the membrane fusion process. Yet, the structural characterization of the interaction of such a protein domain with membrane lipids is still very limited. Therefore, in this work, we present a study of this transmembrane peptide domain in the presence of DMPC membrane bilayers, and we evaluate the effect of several mutations, and the effect of peptide oligomerization in this interaction process. Our results allowed us to identify and confirm amino acid residue motifs that seem to regulate the interaction between the segment peptide and membrane bilayers. Besides these sequence requirements, we have also identified length and tilt requirements that ultimately contribute to the hydrophobic matching between the peptide and the membrane. Additionally, we looked at the association of several transmembrane peptide segments and evaluated their direct interaction and stability inside a membrane bilayer. From our results we could conclude that three independent TM peptide segments arrange themselves in a parallel arrangement, very similarly to what is observed for the C-terminal regions of the hemagglutinin crystallographic structure of the protein, to where the segments are attached.



## INTRODUCTION

Influenza viruses (IV) are responsible for worldwide outbreaks of flu.<sup>1</sup> The most devastating viral infection in the 20th century was not caused by HIV but by the Spanish influenza, which was derived from an IV found in birds. Furthermore, viruses from the 1957 and 1968 pandemics were hybrids between human and avian viruses,<sup>2</sup> and given that humans did not have immunity to avian influenza, these pandemics had devastating consequences.<sup>3</sup> More recently, the new strain of H1N1 IV, which is a combination of genes from swine, avian, and human influenza, spawned the 2009 flu pandemic outbreak, which began in Mexico and rapidly spread all over the world, causing numerous deaths. Therefore, increased knowledge in the understanding of the virus cycle infection is essential to preventing future public flu outbreaks.

The IV hemagglutinin (HA) protein is the best characterized viral protein.<sup>4–10</sup> This protein is a homotrimer, and each subunit in the trimer consists of two polypeptide chains, HA1 and HA2. The protein is first synthesized as a single preprotein

(HA0), which is cleaved by cellular proteases into HA1 and HA2 upon virus maturation and budding at the cell surface. The HA1 chains of the trimeric protein are the globular regions found on top of the protein enclosing the more condensed HA2 subunits, characterized by bundles of helical hairpins with coiled–coiled  $\alpha$ -helical cores. The HA1 chains harbor the sialic acid binding domains responsible for the initial attachment to the cell surface. After these initial events, the virus is internalized into cell endosomes where the low pH triggers a dramatic conformational change in HA (spring loaded model)<sup>5,6</sup> making the HA1 subunit become more separated from HA2 (except for a residual disulfide tether). This leads to a refolding of the HA2 subunit, making the initial protected fusion peptide (FP)<sup>11–13</sup> found in the N-terminus of this subunit exposed and in close contact with the membrane of the endosome. This proximity facilitates the destabilization of the

Received: July 20, 2012

target membrane bilayer by the FP in a process that is still not very well understood.<sup>14</sup> It has also been suggested that the transmembrane peptide (TM) found in the C-terminal of the HA2 subunit,<sup>15–17</sup> besides acting as the anchor of the HA protein to the viral membrane segment peptide, can also play important roles in the budding and in the infection of these viruses. For example, it has been shown that replacing the TM segment peptide with a glycosphosphoinositol-linked lipid anchor, hemifusion (incomplete fusion) is observed.<sup>18</sup> It has also been suggested that the TM peptide is involved in the association of HA proteins in lipid rafts, providing a sufficient concentration of HA to promote viral fusion.<sup>10</sup>

Membrane dehydration has been described to be a key promoter of the fusion of membranes. Interaction studies between a synthetic peptide representing the TM peptide of the HA protein with model membranes revealed that this peptide increases the ordering of lipids<sup>17</sup> and implicitly promotes the dehydration of membranes.<sup>19</sup> This type of dehydration effect has also been identified in works performed with several fusogenic peptides<sup>20</sup> where an increase in the order parameter of the lipid hydrocarbon chains of membranes is observed. Therefore, if we take into account that, during the fusion process observed in IV, the HA proteins adopt a global hairpin structure that brings together both membranes where the FP and the TM peptides are anchored/interacting, this type of dehydration effect will create a hydrophobic region, that ultimately contributes to their fusion. However, and despite all these proposals and suggestions, the structural events associated with them are still not fully conclusive.

The objective of this work is to perform a more accurate characterization of the TM peptide in membrane bilayer environments. Since this segment peptide is quite difficult to structurally characterize using experimental methodologies, molecular dynamics simulations can be seen as a good alternative to perform this type of study. We have performed several simulations of a transmembrane peptide in the presence of a membrane bilayer in order to understand in more detail the structural determinants contributing to the efficient anchorage (interaction with the membrane bilayer) and fusion mechanism of IV (see Figure 1). We have also tested several mutations to

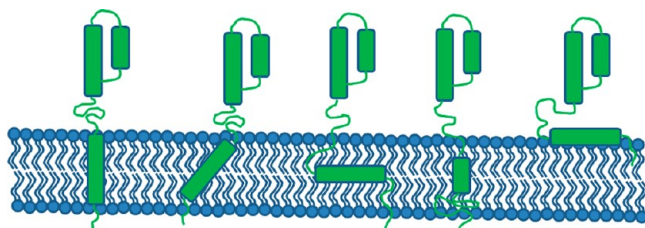


**Figure 1.** Cartoon representation of possible interaction modes of the TM peptide of HA protein with membrane bilayers. One monomer of one monomer of the soluble part of the HA molecule is represented together with the TM peptide.

try to identify possible fusion sequence requirements that could contribute to such efficient event. Finally, we have also looked into the interaction of three different TM peptide segments in order to simulate the natural trimer found in this protein. From our studies, we could see that the TM peptides arrange themselves consistently to the position of the C-terminal regions found in the crystallographic HA protein where the TM will be attached.

## MATERIAL AND METHODS

**Molecular Dynamics Simulation Details.** All simulations were performed with the GROMOS 53A6 force field,<sup>21,22</sup> using the software package GROMACS 4.0.4<sup>23</sup> and with the SPC water model.<sup>24</sup> In the simulations with a membrane bilayer, the charges used in the polar atoms of the lipid molecules were taken from Chiu and co-workers.<sup>25</sup> We have used periodic boundary conditions in a rectangular unit cell in all the simulations with a membrane lipid system and a rhombic dodecahedral unit cell for the simulations in aqueous systems. A twin-range cutoff of 8 Å and 14 Å to short and long interactions was used, respectively. The neighbor list was updated every five steps of simulation. In order to simulate long-range electrostatic interactions, we have used the reaction-field method<sup>26,27</sup> with a dielectric constant of 54. The SETTLE algorithm<sup>28</sup> was used to constrain all the bond lengths of the water molecules, while the LINCS algorithm<sup>29</sup> was used to constrain the bonds of the peptide and lipid molecules. The time step used for integration was 2 fs. We have used three separate Berendsen heat baths to couple the peptide, solvent molecules, and DMPC lipids (in the simulations with lipids), at a temperature of 303 K and with a relaxation time constant of 0.1 ps. For the simulations with aqueous systems, we have used a Berendsen pressure coupling<sup>30</sup> at 1 bar with a relaxation time constant of 0.5 ps and a compressibility of  $4.5 \times 10^{-5} \text{ bar}^{-1}$ . In the simulations with lipids, we have also used a surface tension pressure coupling with a relaxation time constant of 5 ps and a compressibility of  $4.5 \times 10^{-5} \text{ bar}^{-1}$ . The *z* component of the pressure was set to 1 bar, and the *XY* surface tension was 25 dyn/cm. These simulation conditions were shown by Machuqueiro et al.<sup>31</sup> to correctly reproduce several experimental measurements for this type of system. For each simulation condition, we have performed three different replicates by applying different initial velocities. In the aqueous system simulations, we have performed 100 ns for each replicate, while for the simulations with membrane lipids we have performed 500-ns-long simulations.

**Aqueous Simulations Setup and Equilibrations.** We have performed simulations of the TM peptide in three different media. The first one was a medium composed solely of water molecules (10 642). The second one was a medium with only hexane molecules (1310), and the third one was a medium composed by a mixture of both hexane and water (1310 molecules of hexane and 44 984 molecules of water). In all simulations, we have initially placed the TM peptide segment in the center of the simulation box.

The same initialization protocol was used in all simulations. The system was successively minimized by two sets of minimizations with the steepest descent method using 2000 steps. In the first set, we have restrained all the atoms of the peptide, and in the second set, the position restraints were applied to the *C $\alpha$*  atoms only. The force constant applied in both sets of minimization was  $1000 \text{ kJ mol}^{-1} \text{ nm}^{-2}$ .

We have initiated the molecular dynamics simulations by performing 1 ns of simulation with all the atoms of the peptide restrained (force constant of  $1000 \text{ kJ mol}^{-1} \text{ nm}^{-2}$ ) followed by another 1 ns where only the *C $\alpha$*  atoms were restrained. After this initialization time, the rest of the remaining simulation time (98 ns) was performed with an unrestrained system.

**DMPC Membrane Bilayer Setup and Equilibration.** The initial membrane bilayer used in our simulations was composed of 128 DMPC molecules, disposed into two layers of

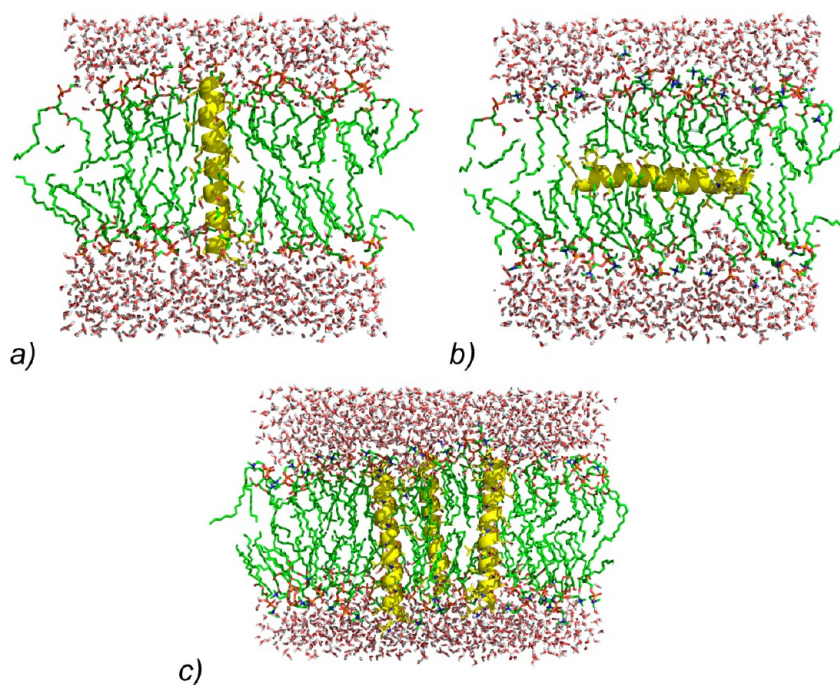


**Figure 2.** Initial setups for the three sets of simulations of the TM peptide inside a membrane bilayer. In a, the TM (colored in yellow) is perpendicular to the plane of the DMPC membrane (in green), while in b, the segment peptide is placed between the two lipid monolayers, parallel to the plane of the membrane bilayer. In c, we present the initial system used in the simulations of the trimer. Image was prepared with PyMOL.<sup>32</sup>

64 molecules. This system was fully hydrated with 4214 water molecules and minimized with 2000 steps of steepest descent, with all the lipid atoms being restrained (with a force constant of  $1000 \text{ kJ mol}^{-1} \text{ nm}^{-2}$ ), followed by another 2000 steps of steepest descent, but now with a force constant of  $100 \text{ kJ mol}^{-1} \text{ nm}^{-2}$ . The molecular dynamics simulation was initiated by performing 1 ns of simulation where harmonic restraints were imposed in all lipidic atoms with a force constant of  $1000 \text{ kJ mol}^{-1} \text{ nm}^{-2}$ , followed by a further 1 ns of simulation with harmonic restraints with a force constant of  $100 \text{ kJ mol}^{-1} \text{ nm}^{-2}$ . After this initiation protocol, we performed 498 ns of fully unrestrained simulation, for a total of 500 ns of simulation.

**Generating the TM Peptide Structure.** In this work, we have used 27 amino acid residues of the sequence of the TM from the H5 subtype (sequence: ILSIYSTVASSLALAIM-VAGLSLWMCS). The residue numbering adopted in the rest of this work takes the first residue in the sequence to be isoleucine 1 and the last to be serine 27. Since no 3D structure (NMR or X-ray crystallography) of the TM peptide is available, we have used the program PyMOL<sup>32</sup> to generate a helical model of such a segment peptide. The protonation states of the side chains of the residues composing the TM peptide were set to their experimental default protonation states at pH 7. Both N and C termini were set to their neutral state in order to mimic the fact that they are peptide bonded to the preceding and following polypeptide domains.

We have also studied the effect of several mutations in the TM peptide when simulated inside a membrane bilayer. The mutations we have studied were selected based on their natural variability (see Figure 8) and based on their reported<sup>33–35</sup> effect in transmembrane segments found in other biological systems. Therefore, the studied mutations were the following: Tyr5Ala, Ser11Ala, Leu14Ala, Trp24Ala, and the double mutant Tyr5Ala–Trp24Ala. All the mutants were prepared using the visualization software PyMOL.<sup>32</sup>

#### Assembling and Simulation of the TM Peptide(s) in the DMPC Membrane Bilayer.

We have performed three different sets of simulations of the TM peptides in the presence of a DMPC membrane bilayer. In the first set, the TM peptide was placed perpendicularly to the plane of the membrane bilayer (Figure 2a). In this set, to avoid atomic clashes between the atoms of the TM peptide and lipids, three DMPC lipids from each monolayer were removed. In the second set of simulations (Figure 2b), we have inserted the TM peptide between the two monolayers of the bilayer, parallel to the plane of the membrane. As previously, in order to avoid clashes between the TM peptide atoms and the atoms of the membrane bilayer, three DMPC lipids were removed from each monolayer. The final set used in our work (Figure 2c) consisted of placing three copies of the TM peptide fully embedded inside a 128 DMPC lipid bilayer perpendicularly to the plane of the bilayer. In this situation, 12 DMPC lipids were removed from the bilayer (six from each monolayer) in order to accommodate the three copies of the TM, without having clashes between different atoms.

In all the sets of simulations with TM peptide(s) and a DMPC membrane bilayer, we have started by fully hydrating the system with 3558 water molecules. Then, each simulation system was minimized with 2000 steps of steepest descent, with all the lipid and peptide(s) atoms being harmonically restrained (with a force constant of  $1000 \text{ kJ mol}^{-1} \text{ nm}^{-2}$ ), followed by another 2000 steps of steepest descent, but now with a force constant of  $100 \text{ kJ mol}^{-1} \text{ nm}^{-2}$ . The molecular dynamics simulations were initiated by performing 1 ns of simulation where harmonic restraints were imposed on all lipidic and peptide(s) atoms with a force constant of  $1000 \text{ kJ mol}^{-1} \text{ nm}^{-2}$ , followed by a further 1 ns of simulation with harmonic restraints with a force constant of  $1000 \text{ kJ mol}^{-1} \text{ nm}^{-2}$ , but now only applied to the atoms of the peptide(s). Following these two steps, we have performed a further 8 ns of simulation,



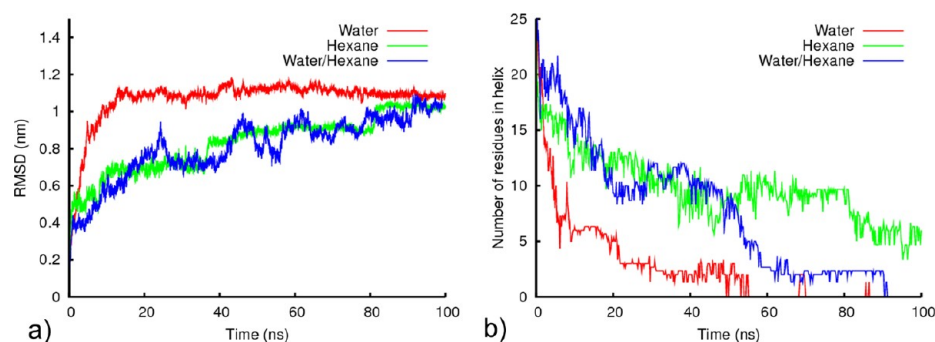


**Figure 3.** Stability of the TM helices in water, hexane, and water/hexane media, showing the average Cα RMSD to the initial structure (a) and the average number of residues with helical arrangement (b).

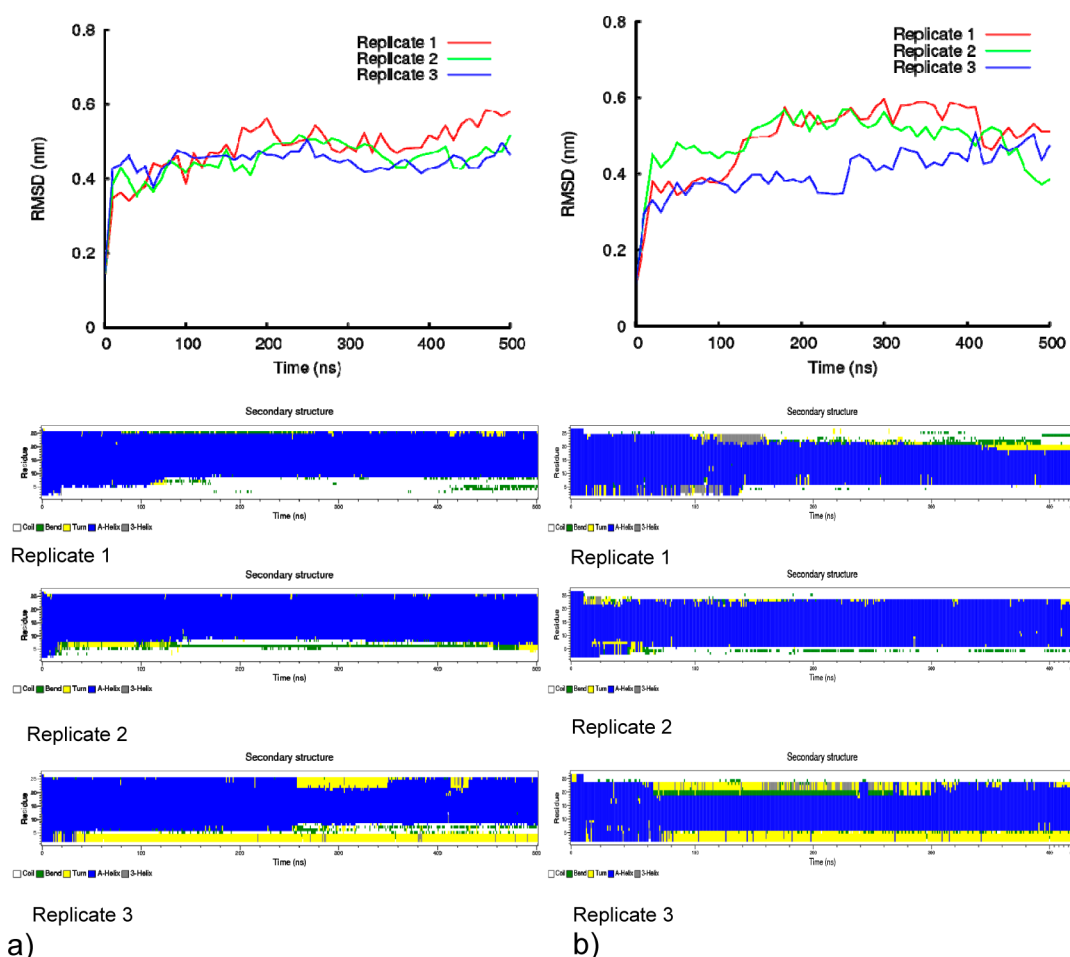


**Figure 4.** RMS deviation from the initial structure of the TM peptide and DSSP plots of the peptides throughout simulation time, when it starts perpendicular (a) or parallel (b) to the membrane plane. The plots display the results of the three replicate simulations for each set.

where a harmonic restraint with a force constant of  $1000 \text{ kJ mol}^{-1} \text{ nm}^{-2}$  was applied to only the Cα atoms of the TM peptide(s). After this initiation protocol, we have performed 490 ns of fully unrestrained simulation, for a total of 500 ns of simulation.

The protocol used to insert and simulate the mutant peptides in the membrane bilayer was the same as described previously for the wild-type TM peptide(s).

## RESULTS AND DISCUSSION

**Stability of the TM Segment Peptide in Water, Hexane, and Water/Hexane Mediums.** We have started

our work by performing an evaluation of the secondary arrangement of the TM peptide based on its amino acid sequence, using the Phyre Web site.<sup>36</sup> According to the submitted data, the 27 residues composing the TM peptide were shown to favor a helical fold. In order to further characterize the peptide and to gather information about the stability of the TM peptide segment in media with different hydrophobicity properties, we have carried out MD simulations of the TM peptide as a helix (100 ns each). For each simulation condition (water, hexane and water/hexane), we have performed three replicate simulations with the TM peptide, in a total of nine simulations.

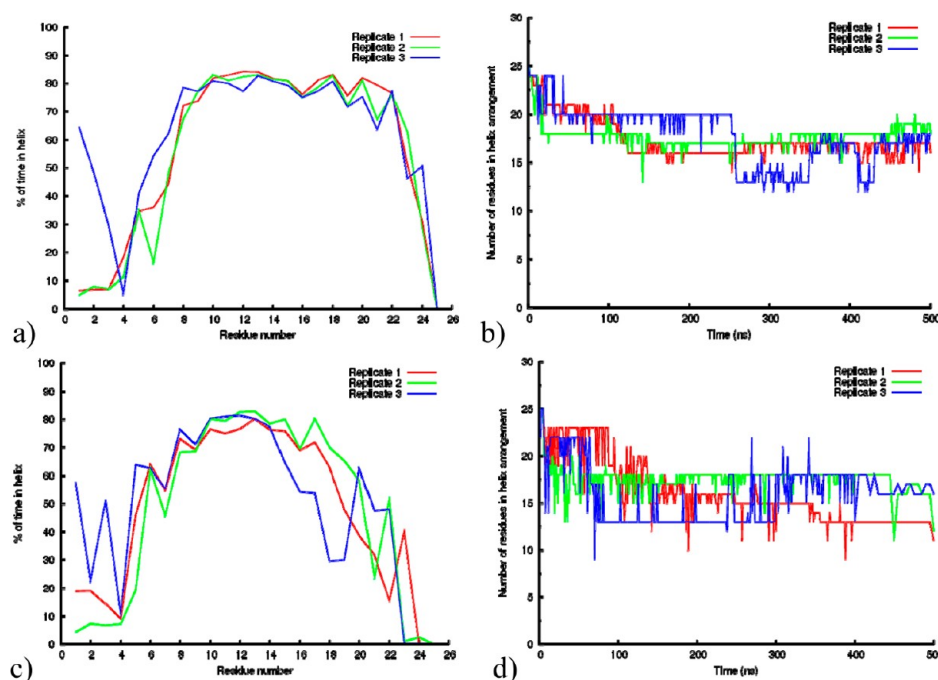


**Figure 5.** In a and c, the percentage of time spent by each residue as a helix for the simulations where the TM peptide was initially placed perpendicularly and parallel to the plane of the membrane, respectively. In b and d, we show the variation of the number of residues in helix arrangement over time, again for both sets of simulations. All measurements presented in this figure were done using the GROMACS tool `g_helix`. All these analyses were done excluding the first 10 ns of simulation, from where we considered that the system was still equilibrating.

As can be seen in Figure 3, after 100 ns of simulation, the TM peptide loses its helical fold in all three media. However, the time scale for these unfolding events is different, depending on the simulated medium. In the pure water simulations, the initial helical fold of the TM peptide was completely lost after 10 ns of simulation. In fact, this is expected, since hydrophobic helices are not expected to be stable in hydrophilic media.

When the simulations are performed in a pure hydrophobic medium such as hexane, the unfolding behavior in the first nanoseconds of simulation time is different from what is observed in water. Despite considerable destruction of the structure, the initial helical fold in this medium is not entirely lost after 100 ns of simulation, with five residues remaining helical. Similarly, in the simulations with a medium composed by the mixture of water and hexane, we can see that until nanosecond 50, the evolution of the helical content is very similar to the one observed for the pure hexane medium. However, after 50 ns the helical fold of the TM peptide is completely lost in a similar way to that observed for the simulations in pure water. Interestingly, all simulations in this mixture showed the peptide spending most of the time at the water/hexane interface, as illustrated in Figure S1. This observation is not what we were expecting initially since we are dealing with a peptide mostly composed of hydrophobic residues. Since the peptide segment could be divided into two distinct parts, depending on the amino acid residue composition (the N-terminal region is more hydrophilic, when compared to the C-terminal), we would expect to find the more hydrophilic part of the peptide to be embedded in the more hydrophilic part of the medium (water) while the hydrophobic part of the segment peptide embedded in the more hydrophobic region (hexane). However, this was not observed. The unfolding process evidenced by the TM in this set of simulations made the peptide segment lose its initially

clear hydrophilic–hydrophobic profile. Consequently, the observed preferred position of the peptide segment was the interface between the two media (Figure S1).

Overall, from these simulations we could conclude that the TM peptide, independently of the simulated media, loses most of its initial helical fold after 100 ns of simulation. Although this unfolding event is faster in pure water media, it is also observed under the other simulated conditions. Therefore, and based on these conclusions, we decided to do the evaluation of the stability of the TM peptide in a more physiological medium, such as the DMPC membrane bilayer.

**Stability of the TM Segment Peptide Inside a DMPC Membrane Bilayer.** As mentioned previously in the Material and Methods section, in order to study the stability of the TM peptide when embedded in a lipid DMPC membrane bilayer, we have performed two sets of simulations, where the TM peptides were placed in two different arrangements inside a membrane bilayer (see Figure 2). With these two different starting positions of the TM peptide in the DMPC membrane bilayer, we wanted to see how this segment peptide behaves and arranges itself inside the membrane, independently of its starting conformation.

In a first overall evaluation of both sets of simulations, we were able to see that, independently of the starting conformation, the TM peptide was able to keep a much more helical structure than in the simulations performed solely in water, hexane, and water/hexane.

As can be seen in Figure 4, a consistent increase in the deviation from the initial structure is observed. Independently of the starting conditions, the variation of the RMSD values is very similar, which may indicate that the level of conformational variability in the two sets of simulations could be identical. In order to identify in more detail the regions of the segment peptide contributing to the increase in the RMSD, we

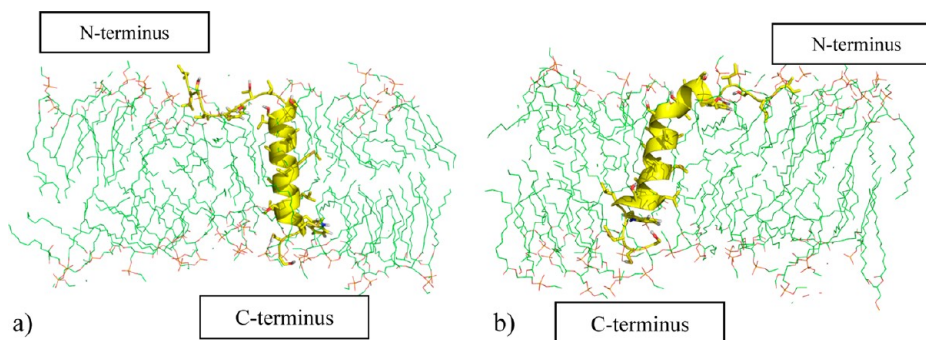


**Figure 6.** Final snapshot of a simulation replicate started with a perpendicularly (a) and parallelly (b) oriented peptide. N-terminal amino acids uncoil, while the region more embedded in the membrane bilayer stays as a helix. This figure was built using the software PyMOL.<sup>32</sup>

plotted (Figure 5) the variation of the number of residues in a helical arrangement versus the simulation time, and also the percentage of simulation time spent by each residue in helical fold. The evaluation of the helicity and its relation to the function of TM peptide segments has been a highly debated theme in recent years.<sup>33</sup> In order to perform a good evaluation of the stability and of the conformational variability of the TM peptide segment inside the membrane lipid bilayer, we have looked into several helical properties.

As can be seen in Figure 5 and in the DSSP plots in Figure 4, the main explanation for the increase in the RMSD values in our simulations was the unfolding of the helix at both terminal regions of the peptide. Overall, the average number of residues in helical fold is slightly lower in the parallel when compared with the perpendicular simulations (Figure 5b and d). While the simulations where the peptide starts with a perpendicular orientation exhibit an average of 17 residues in helical arrangement, that number decreases to 15 when it starts with a parallel orientation. This seems to be due to differences in the C-termini, probably due to the “unstable” initial conformation of the parallel simulations. Nevertheless, it is remarkable that the final position of the TM peptide in both sets of simulations is very similar, considering the radically different initial configuration. In both sets of simulations, the N and C terminals of the TM peptide rapidly rearrange and settle at the membrane interface (Figures S3 and S4 present the final snapshots of all the replicate simulations for both sets).

As mentioned above, the loss of helical fold in the simulations started with a perpendicularly oriented peptide that is higher at the N-terminus (seven residues) than at the C-terminus (five residues). This is illustrated in Figure 6, where the final snapshot of a replicate from this set of simulations is represented, and where the accommodation of the TM peptide segment to the membrane bilayer is evident. During this process, the initial seven residues found in the N-terminal region of the peptide lose their helical fold and become more exposed to the solvent. This event resulted in an increase in the number of interactions with water molecules in the solution (results not shown) and with the polar interfacial region of the membrane bilayer. A similar but less extensive unfolding is observed in the C-terminus. By carefully looking at Figure 6, we can identify two aromatic residues (a tyrosine residue at position 5 and a tryptophan at position 24) that seem to act as helical delimiters that preclude the unfolding. Interestingly, it has been reported<sup>37</sup> that in this type of transmembrane peptide there is a high probability of finding aromatic amino acid residues, such as tyrosines, tryptophans, or phenylalanines, in interfacial regions of the membrane bilayer. For example, in

WALP peptides,<sup>37</sup> tryptophan amino acids found in interfacial positions of membrane proteins and peptides are proposed to anchor transmembrane segments to the membrane. These types of residues show a high propensity for being found in the interfacial regions and are also known to inhibit the tilting of TM segments. This behavior can be understood mainly due to two reasons. First, interfacial tryptophan residues were found to order lipids in the vicinity of TM segments when experiencing a positive hydrophobic mismatch, which may indicate a concerted response of the lipids around the TM segments that ultimately hinders their tilting.<sup>37</sup> On the other hand, it was found that tryptophans prefer certain locations at the membrane interface that could be important to maintaining the correct localization and orientation of these residues at the membrane/water interface.<sup>38</sup> These proposals are also supported by our simulations. As can be seen in Figures S3 and S4 (where the final snapshots of all replicates in both simulations sets are presented), both Tyr5 and Trp24 are found close to both terminals of the TM peptide, becoming close or actually at the interface of the membrane bilayer. This is also observed during the simulations (results not shown), where a rapid migration of these two residues from their initial position in the bilayer is observed.

As previously mentioned, on average, 17 residues of the TM peptide segment are found in a helical arrangement (between residue 7 and residue 24, Figure 6). According to several authors,<sup>16,37,39</sup> this number of amino acid residues in helical arrangement is the minimum number that efficiently promotes the hemifusion-to-fusion transition. These authors also reported that 16-residue-long peptide segments of HA TM severely impair the hemifusion-to-fusion process, while 15-residue-long peptides fully arrest the membrane fusion process at the hemifusion step. Taking these facts into account, together with our observations in the simulations, we can conclude that the TM peptide used here, approximately 17 residues long in a helical arrangement, would be fully competent for anchoring the HA protein to the membrane and likely promote full membrane fusion.

As illustrated in Figure 6, helical loss is also observed in the simulations started with the peptide oriented parallel to the membrane, with the helix spanning from tyrosine 5 to leucine 20 (Figure 5c). Relative to the perpendicular case, this loss is similar at the N-terminus but larger at the C-terminus, although the tryptophan residue at position 24 remains at the lipid/water interface and may thus control the peptide orientation and helical extent.

Another important property of transmembrane peptides is tilting, which occurs to avoid a hydrophobic mismatch between



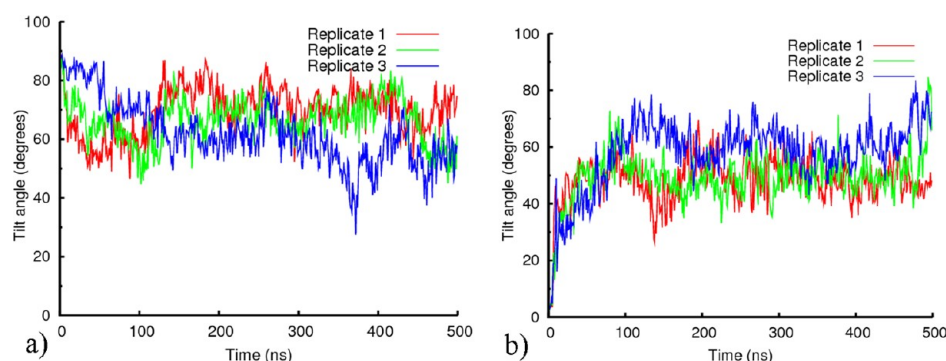


**Figure 7.** Temporal evolution of the tilt angle between the TM peptide helical axis and the plane of the membrane, for the sets of simulations started with the helix in a perpendicular (a) and parallel (b) orientation relative to the plane. To plot these results, we have calculated the angle between the vector represented by the residues of the peptide in a helix and the plane formed by the phosphorus atoms of the lipids in the upper bilayer.

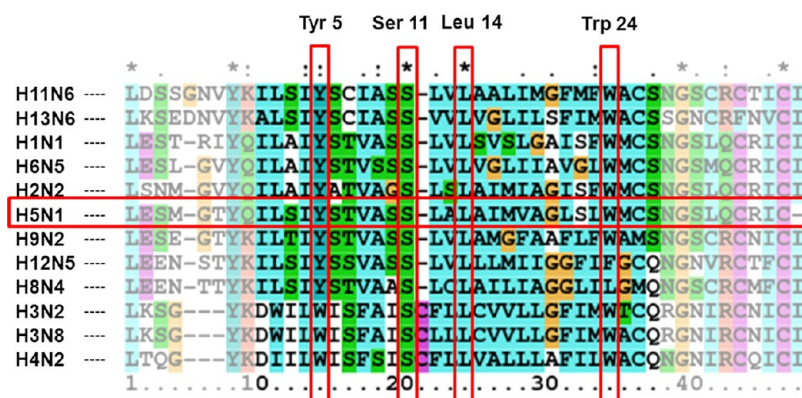


**Figure 8.** Sequence alignment (using ClustalX<sup>47</sup>) between the TM peptide segments of different HA subtypes. The horizontal red rectangle indicates the sequence of the HA TM peptide subtype we are using in this study, while the vertical rectangles indicate the residues we have mutated.

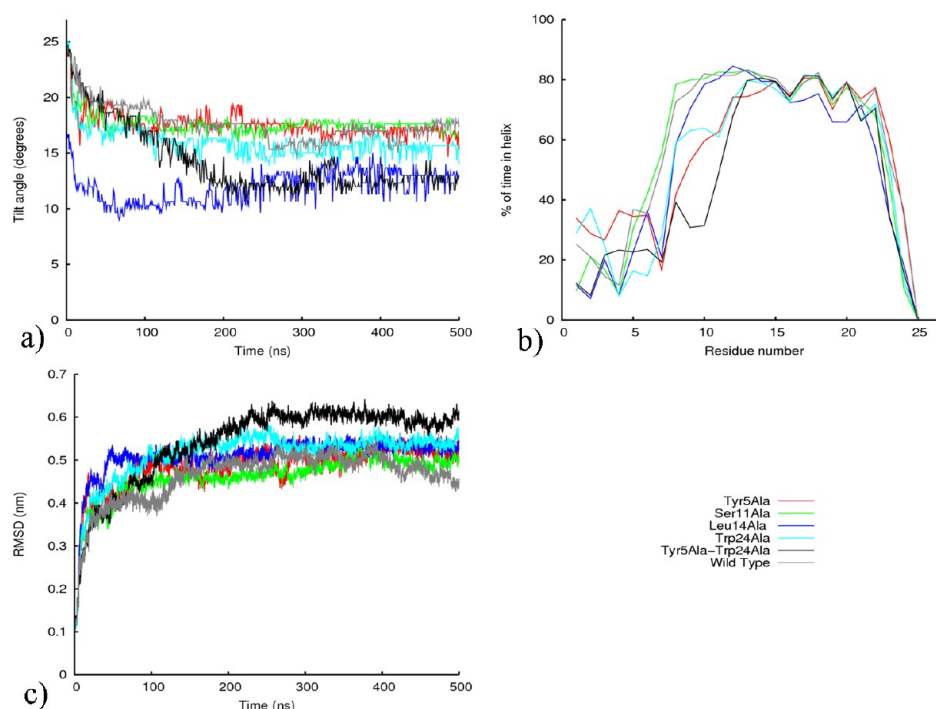


**Figure 9.** (a) Average variation of the number of residues with an  $\alpha$ -helix topology along time, (b) average percentage of time that each residue spends in the helix, (c) average RMSD over time. The plots contain results concerning the wild type and mutant simulations. Averages are taken over replicates.

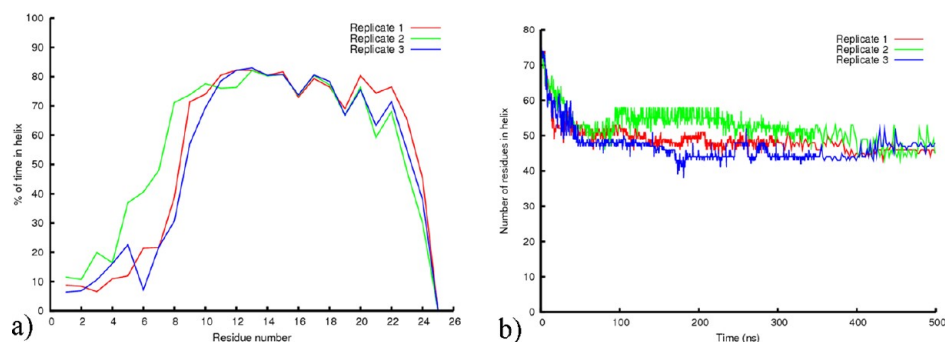


**Figure 10.** Figure a presents the average helicity per residue of all three TM peptide segments of the trimer for all three replicate simulations. In b, we show the average variation of the number of residues of all the TM peptide segments of the trimer throughout simulation times.

the peptide and the lipid environment. As can be seen in Figure 7, in the simulations started with the perpendicularly oriented peptide, the TM peptide achieves a tilt angle that varies between 50 and 80° (when the tilt angle is close to 90°, it is perpendicularly aligned to the plane of the membrane). This tilt angle range is also similar to the range obtained at the end of the simulations started with the peptide in a parallel orientation (i.e., with a tilt angle of zero degrees; Figure 7b), although in this case the differences between the three simulations is larger. Therefore, in both sets of simulations, the peptide rapidly evolves to tilt angles that are, on average, around 60°, which is in agreement with previous reports.<sup>17,19,37</sup> As noted in several recent works,<sup>15,16,19,33,39–41</sup> the way that TM segments of proteins and peptides span over the membrane bilayer may highly influence their function. Interestingly, it has also been reported that in order to promote an efficient fusion process, TM peptide segments should adopt a minimum segment length<sup>39</sup> and also a certain tilting across that membrane bilayer.<sup>42</sup> One possible justification for this fact could come from the observation that the TM segments play an important role in the disruption of the lipid bilayers during the fusion process.<sup>17,35</sup> Since the bilayer disruption by the TM peptides critically depends on the extent of the matching between the peptide length and the bilayer thickness,<sup>43,44</sup> an unstable insertion of small TM peptide segments could lead to their inability to disturb the hemifusion diaphragm.<sup>39</sup> Another possibility could be that, to facilitate the membrane fusion process, the TM peptide segment applies a tension on the membrane so that it may break the hemifusion diaphragm and consequently promote pore formation.<sup>45</sup> If a correct span is not obtained, the ability for a short TM peptide segment to be able to apply such a tension is unlikely, which overall results in an inability to promote the membrane fusion.

**Stability of the TM Mutants Inside a DMPC Membrane Bilayer.** Having determined the arrangement of a wild type TM peptide in a model membrane, we wanted to go further and test the importance of several amino acid residues in this process. The first approach to inferring the relative importance of different residues in TM peptides is to look at their natural variability, which is presented in Figure 8, which contains a sequence alignment of TM peptides from different HA subtypes. The first observation from Figure 8 is the considerably high homology between the different subtypes of HA, a fact reported before.<sup>41</sup> We used this knowledge, together with the position of specific amino acids in the TM transmembrane topology found in the simulations, to select five different mutants: Tyr5Ala, Ser11Ala, Leu14Ala, Trp24Ala, and the double mutant with Tyr5Ala and Trp24Ala. The Tyr5Ala

and Trp24Ala were selected since these two residues have characteristics to act as peptide delimiters at the interface of the membrane bilayer.<sup>37,41,46</sup> Ser11 and Leu14 were selected since these are the two residues fully conserved in the set of HA subtypes analyzed (see Figure 8). Other reports have also identified these residues as good targets to evaluate the stability of the TM peptide inside membrane bilayers.<sup>33–35</sup>

In Figure 9, we present several properties of the TM peptide inside a membrane bilayer, obtained from the wild type and the different mutants simulations. Concerning the number of residues in the helix over time (Figure 9a), with the exception of Leu14Ala and the double mutant (Tyr5Ala–Trp24Ala), all the remaining mutants show very similar behavior when compared to the wild type. The Leu14Ala mutant shows a rapid decrease in the number of residues in the helix in the first nanoseconds of simulation. For the double Tyr5Ala–Trp24Ala mutant, this decrease is slower than for the previous mutant, but it reaches similar values of helicity, with a 20% decrease from the wild type simulation. However, by looking at Figure 8b, we can see quite distinct helical profiles for these two mutants. The rapid decrease in the helical content for the Leu14Ala simulations is a consequence of the loss of helicity in the region comprising residues 14 to 27, i.e., the C-terminus region. This observation is in agreement with previous authors that state that the substitution of leucine residues in TM peptide segments decreases the stability of helices<sup>34</sup> and consequently membrane fusion.<sup>33</sup> In contrast, in the double mutant Tyr5Ala–Trp24Ala, the most affected region of the peptide is the one near the N-terminus, up to residue 13. The double mutant is more affected in terms of global structure than the single mutants, as confirmed by the RMSD plots in Figure 9c.

The Tyr5Ala mutant is also highly affected, mainly in the N-terminal region (Figure 9b). Additionally, its degree of helicity is higher in the C-terminal region than the wild type, especially in the last four residues. Interestingly, the N-terminal helix destabilization is also evident in the Trp24Ala mutant, whose mutation is in the C-terminal. It seems that the absence of both anchoring aromatic residues leads to helix loss at the N-terminus, something that corroborates the suggestions of other authors concerning TM peptide delimiting residues.

As mentioned in the previous section of this work, the evaluation of the tilting of the TM peptides inside the membrane bilayer is also very important, since this property can be directly related with the stability and function of the TM peptide segments. As previously seen in Figure 7, the average tilting of the wild type TM peptide varies between 60° and 70°, with respect to the plane of the membrane bilayer. As can be



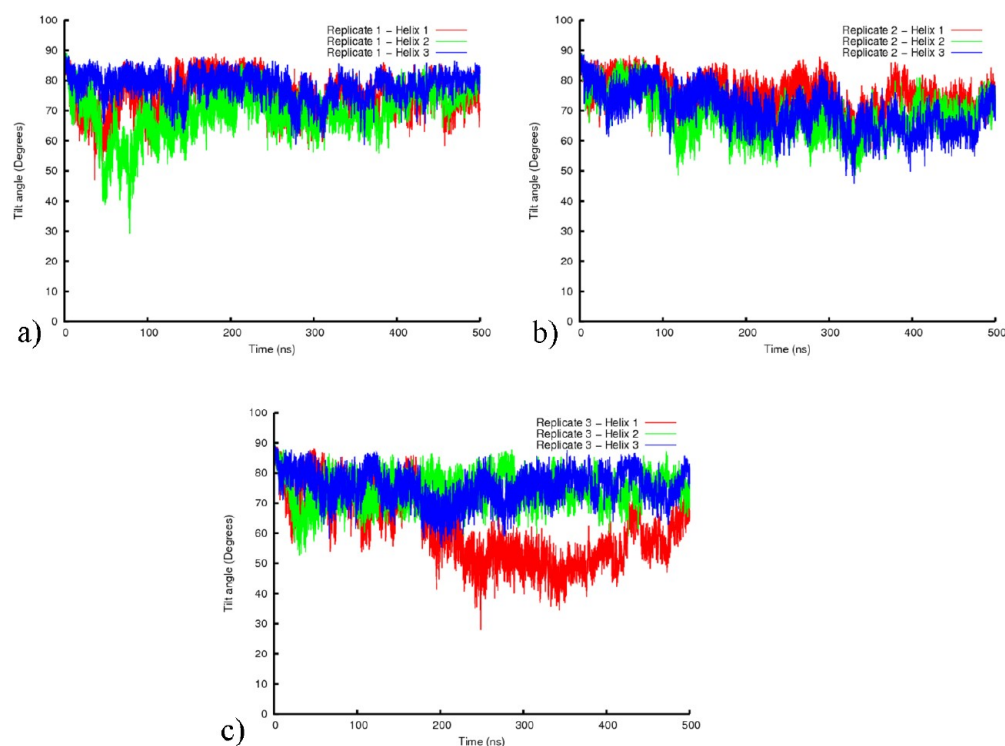


**Figure 11.** Tilt angle over time for the three segment peptides in the trimer simulations for all the replicate simulations.

seen in Figure S5, the final observed average tilting for all the mutant simulations is very similar, as well as the temporal behavior of this property, with the exception of the Ser11Ala mutant (but its final value is similar). Overall, it seems that the tested mutations do not influence the tilting of the membrane peptides inside the membrane bilayers. This type of observation has also been observed in past works done with WALP peptides.<sup>46</sup>

**Stability of the Three-Helix TM Trimer Bundle Inside a DMPC Membrane Bilayer.** The TM peptide is naturally present as a trimer since each of the three subunits of the HA protein are found in a fully functional system.<sup>48–50</sup> Given this, it is interesting to do equivalent studies to the ones reported for the single TM peptide with the trimer embedded in a membrane bilayer.

These simulations were started by placing three different peptide segments inside a previously equilibrated membrane bilayer. All these segments were free to move in the membrane bilayer; i.e., they had no restraints between them. An overall analysis (Figure 10) of these simulations shows that the behavior of the peptides is similar to the behavior found in the single peptide simulations. If we compare Figure 10a with the results presented in Figure 5a, we see that the residues showing a higher percentage of time in the helix are approximately the same, corresponding to a 17 residue segment spanning from residue 7 to 24. Again, the first seven residues of the N-terminus and the last three residues in the C-terminus lose their helical fold during the course of the simulations. Therefore, even if the peptides interact (see below), they do not affect each other's conformation.

In Figure 11, the variation of the tilt angle of the peptide is represented for all peptides in all replicate simulations. As can be seen, although some peptides in different replicates show large fluctuations in the tilt angle, on average, the three peptide segments do present a tilt angle ranging between 70° and 80°

relative to the plane of the membrane. This is approximately 10° higher than the 60–70° range observed in the simulations of a single peptide. This difference could mean that the three TM peptide segments are, on average, more perpendicular relative to the plane of the membrane when compared to the simulations with the single peptides. Although we could not observe a direct interaction between the three TM peptide segments, it seems that each individual segment influences indirectly its neighbor's position in the membrane bilayer.

As illustrated in Figure 12a, although the helical regions of the TM peptide segments do not interact directly, the three helices arrange themselves in close proximity, remaining at a distance of 1.6–2.5 Å from each other during the simulation (see Figure S6). The N-terminal regions lose their helical arrangement (such as previously described for the simulations

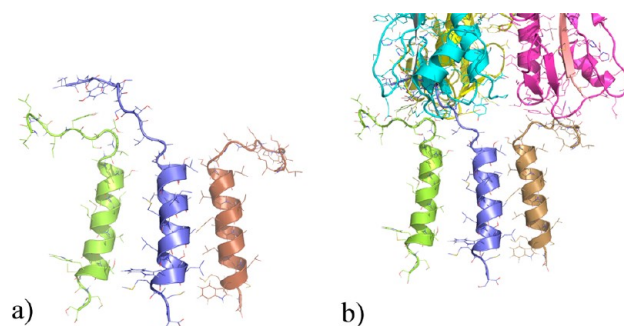


**Figure 12.** In a, the final snapshot of a TM peptide trimer conformation. In b, the same conformation of the TM trimer is presented together with part of the crystallographic structure of HA (top part of the figure). The arrangement between these two objects was obtained by manual fit of the HA crystallographic structure and of the trimer of the TM peptide segment. Both these figures were produced using PyMOL.<sup>32</sup>

with a single peptide) and, occasionally, interact directly with the equivalent regions from neighbor peptide segments, resembling a hook. These regions, previously named linkers, correspond to the beginning of the transmembrane peptide and, depending on the virus subtype HA, are suggested to adopt different quaternary arrangements.<sup>51</sup> As proposed by Kordyukova et al.,<sup>51</sup> these regions may be responsible for resistance of the virus against proteolytic enzymes, and also for a tighter association between the segments and a consequent stabilization of the protein. Since these protein regions show a low content of aromatic residues, known to confer tight associations, the interactions are done by polar (like serine) and some aliphatic residues (like alanines).

Another interesting aspect that should be mentioned concerns the arrangement of the individual segments relative to each other (see Figure 12). The three peptides assemble in a triangular arrangement that approximately matches the positions where they should attach to the structure of HA, here represented by its crystallographic conformation (Figure 12b). Therefore, their arrangement in the membrane is adequate for the attachment of HA, even though the rest of the protein was not included in the simulations.

## CONCLUSIONS

In this work, we were able to conclude that helical TM peptide segments of the HA protein are extremely unstable when incorporated in water, hexane, and a mixture of water–hexane. However, when inserted in an explicit membrane bilayer, the TM peptide becomes mostly helical (17 residues out of 27). In order to get a hydrophobic matching between the TM peptide length and the membrane bilayer thickness, this segment peptide adopts a tilt angle of approximately 64°, which is in agreement with several experimental works. In order to identify key residues that could account for the helicity of this peptide, we have tested the effect of several mutations on its stability when embedded in membrane bilayers. From our results, we were able to identify that the mutations of Trp 24 and Tyr 5 found in the C-terminal and N-terminal regions, respectively, affect the helicity and consequently the peptide arrangement inside the membrane bilayer. This is also in agreement not only with what has been described for this segment peptide but also with several other transmembrane segments found in similar systems. Since the fully functional HA protein is a trimer, we have also performed a set of simulations with three copies of the TM peptide embedded in a membrane bilayer. The results concerning the arrangement of the individual peptides of the trimer are very similar to the ones obtained for the monomer simulations. Furthermore, the three TM peptides arrange themselves in a triangular association, which is in agreement with the position of the C-terminal regions found in the HA2 segment of the HA protein, where the TM peptides are attached.

In conclusion, with this work we were able to test several hypotheses that were previously proposed and contribute overall to a better structural characterization of the way the TM peptide interacts with an explicit membrane bilayer, and its attachment to the soluble part of the protein. The TM peptide exhibits molecular characteristics that allow for a helical insertion in a membrane and its interaction with other TM peptides of HA, even without the presence of the rest of the protein. Therefore, this can by itself be a factor influencing the trimerization of the full HA protein.

## ASSOCIATED CONTENT

### Supporting Information

Snapshot of the TM peptide in a mixed media of water and hexane, DSSP plots of the TM peptide in different media, final snapshots of the TM peptide inside the membrane, average tilting angles of the TM peptide relative to the membrane for the wild-type and mutant simulations, and plots of the distances between the three TM peptide segments obtained during the simulations. This information is available free of charge via the Internet at <http://pubs.acs.org>.

## AUTHOR INFORMATION

### Corresponding Author

\*Telephone: +351 21 4469610. Fax: +351 21 4433644. E-mail: [claudio@itqb.unl.pt](mailto:claudio@itqb.unl.pt).

### Notes

The authors declare no competing financial interest.

## ACKNOWLEDGMENTS

This work was supported by grant with reference PTDC/QUI-BIQ/114774/2009 and by fellowship with reference SFRH/BPD/29708/2006 from FCT (Fundação para a Ciência e a Tecnologia).

## REFERENCES

- (1) Laver, G.; Garman, E. Virology. The origin and control of pandemic influenza. *Science* **2001**, *293*, 1776–1777.
- (2) Zambon, M. C. The pathogenesis of influenza in humans. *Rev. Med. Virol.* **2001**, *11*, 227–241.
- (3) Nichol, S. T.; Arikawa, J.; Kawaoka, Y. Emerging viral diseases. *Proc. Natl. Acad. Sci. U. S. A.* **2000**, *97*, 12411–12412.
- (4) Bizebard, T.; Gigant, B.; Rigolet, P.; Rasmussen, B.; Diat, O.; Bosecke, P.; Wharton, S. A.; Skehel, J. J.; Knossow, M. Structure of Influenza-Virus Hemagglutinin Complexed with a Neutralizing Antibody. *Nature* **1995**, *376*, 92–94.
- (5) Carr, C. M.; Chaudhry, C.; Kim, P. S. Influenza hemagglutinin is spring-loaded by a metastable native conformation. *Proc. Natl. Acad. Sci. U. S. A.* **1997**, *94*, 14306–14313.
- (6) Carr, C. M.; Kim, P. S. A Spring-Loaded Mechanism for the Conformational Change of Influenza Hemagglutinin. *Cell* **1993**, *73*, 823–832.
- (7) Korte, T.; Ludwig, K.; Huang, Q.; Rachakonda, P. S.; Herrmann, A. Conformational change of influenza virus hemagglutinin is sensitive to ionic concentration. *Eur. Biophys. J. Biophys. Lett.* **2007**, *36*, 327–335.
- (8) Madhusoodanan, M.; Lazaridis, T. Investigation of pathways for the low-pH conformational transition in influenza hemagglutinin. *Biophys. J.* **2003**, *84*, 1926–1939.
- (9) Stevens, J.; Corper, A. L.; Basler, C. F.; Taubenberger, J. K.; Palese, P.; Wilson, I. A. Structure of the uncleaved human H1 hemagglutinin from the extinct 1918 influenza virus. *Science* **2004**, *303*, 1866–1870.
- (10) Takeda, M.; Leser, G. P.; Russell, C. J.; Lamb, R. A. Influenza virus hemagglutinin concentrates in lipid raft microdomains for efficient viral fusion. *Proc. Natl. Acad. Sci. U. S. A.* **2003**, *100*, 14610–14617.
- (11) Chang, D. K.; Cheng, S. F.; Trivedi, V. D.; Yang, S. H. The amino-terminal region of the fusion peptide of influenza virus hemagglutinin HA2 inserts into sodium dodecyl sulfate micelle with residues 16–18 at the aqueous boundary at acidic pH - Oligomerization and the conformational flexibility. *J. Biol. Chem.* **2000**, *275*, 19150–19158.
- (12) Lai, A. L.; Park, H.; White, J. M.; Tamm, L. K. Fusion peptide of influenza hemagglutinin requires a fixed angle boomerang structure for activity. *J. Biol. Chem.* **2006**, *281*, 5760–5770.

- (13) Sammalkorpi, M.; Lazaridis, T. Configuration of influenza hemagglutinin fusion peptide monomers and oligomers in membranes. *Biochim. Biophys. Acta, Biomembr.* **2007**, *1768*, 30–38.
- (14) Fuhrmans, M.; Marrink, S. J. Molecular View of the Role of Fusion Peptides in Promoting Positive Membrane Curvature. *J. Am. Chem. Soc.* **2012**, *134*, 1543–1552.
- (15) Langosch, D.; Hofmann, M.; Ungermann, C. The role of transmembrane domains in membrane fusion. *Cell. Mol. Life Sci.* **2007**, *64*, 850–864.
- (16) Schroth-Diez, B.; Ludwig, K.; Baljinnyam, B.; Kozerski, C.; Huang, Q.; Herrmann, A. The role of the transmembrane and of the intraviral domain of glycoproteins in membrane fusion of enveloped viruses. *Biosci. Rep.* **2000**, *20*, 571–595.
- (17) Tatulian, S. A.; Tamm, L. K. Secondary structure, orientation, oligomerization, and lipid interactions of the transmembrane domain of influenza hemagglutinin. *Biochemistry* **2000**, *39*, 496–507.
- (18) Scolari, S.; Engel, S.; Krebs, N.; Plazzo, A. P.; De Almeida, R. F. M.; Prieto, M.; Veit, M.; Herrmann, A. Lateral Distribution of the Transmembrane Domain of Influenza Virus Hemagglutinin Revealed by Time-resolved Fluorescence Imaging. *J. Biol. Chem.* **2009**, *284*, 15708–15716.
- (19) Chang, D. K.; Cheng, S. F.; Kantchev, E. A. B.; Lin, C. H.; Liu, Y. T. Membrane interaction and structure of the transmembrane domain of influenza hemagglutinin and its fusion peptide complex. *BMC Biol.* **2008**, *6*, 2.
- (20) Han, X.; Steinhauer, D. A.; Wharton, S. A.; Tamm, L. K. Interaction of mutant influenza virus hemagglutinin fusion peptides with lipid bilayers: Probing the role of hydrophobic residue size in the central region of the fusion peptide. *Biochemistry* **1999**, *38*, 15052–15059.
- (21) Oostenbrink, C.; Villa, A.; Mark, A. E.; van Gunsteren, W. F. A biomolecular force field based on the free enthalpy of hydration and solvation: the GROMOS force-field parameter sets 53A5 and 53A6. *J. Comput. Chem.* **2004**, *25*, 1656–1676.
- (22) Scott, W. R.; Hunenberger, P. H.; Tironi, I. G.; Marck, A. E.; Billeter, S. R.; Fennen, J.; Torda, A. E.; Huber, T.; Kruger, P.; van Gunsteren, W. F. The GROMOS Biomolecular Simulation Program Package. *J. Phys. Chem. A* **1999**, *103*, 3596–3607.
- (23) Hess, B.; Kutzner, C.; van der Spoel, D.; Lindahl, E. GROMACS 4: Algorithms for highly efficient, load-balanced, and scalable molecular simulation. *J. Chem. Theory Comput.* **2008**, *4*, 435–447.
- (24) Hermans, J.; Berendsen, H. J. C.; Vangunsteren, W. F.; Postma, J. P. M. A Consistent Empirical Potential for Water-Protein Interactions. *Biopolymers* **1984**, *23*, 1513–1518.
- (25) Chiu, S. W.; Clark, M.; Balaji, V.; Subramaniam, S.; Scott, H. L.; Jakobsson, E. Incorporation of Surface-Tension into Molecular-Dynamics Simulation of an Interface - a Fluid-Phase Lipid Bilayer-Membrane. *Biophys. J.* **1995**, *69*, 1230–1245.
- (26) Barker, J. A.; Watts, R. O. Monte-Carlo Studies of Dielectric Properties of Water-Like Models. *Mol. Phys.* **1973**, *26*, 789–792.
- (27) Tironi, I. G.; Sperb, R.; Smith, P. E.; Vangunsteren, W. F. A Generalized Reaction Field Method for Molecular-Dynamics Simulations. *J. Chem. Phys.* **1995**, *102*, 5451–5459.
- (28) Miyamoto, S.; Kollman, P. A. Settle - an Analytical Version of the Shake and Rattle Algorithm for Rigid Water Models. *J. Comput. Chem.* **1992**, *13*, 952–962.
- (29) Smith, K. C.; Honig, B. Evaluation of the Conformational Free-Energies of Loops in Proteins. *Proteins: Struct., Funct., Genet.* **1994**, *18*, 119–132.
- (30) Berendsen, H. J. C.; Postma, J. P. M.; van Gunsteren, W. F.; DiNola, A.; Haak, J. R. Molecular dynamics with coupling to an external bath. *J. Chem. Phys.* **1984**, *81*, 3684–3690.
- (31) Machuqueiro, M.; Campos, S. R. R.; Soares, C. M.; Baptista, A. M. Membrane-Induced Conformational Changes of Kyotorphin Revealed by Molecular Dynamics Simulations. *J. Phys. Chem. B* **2010**, *114*, 11659–11667.
- (32) DeLano, W. L. *The Pymol Molecular Graphics System, 0.90*; DeLano Scientific LLC: San Carlos, CA, 2003.
- (33) Hofmann, M. W.; Weise, K.; Ollesch, J.; Agrawal, P.; Stalz, H.; Stelzer, W.; Hulsbergen, F.; de Groot, H.; Gerwert, K.; Reed, J.; Langosch, D. De novo design of conformationally flexible transmembrane peptides driving membrane fusion. *Proc. Natl. Acad. Sci. U. S. A.* **2004**, *101*, 14776–14781.
- (34) Lorin, A.; Charlotiaux, B.; Fridmann-Sirkis, Y.; Thomas, A.; Shai, Y.; Brasseur, R. Mode of membrane interaction and fusogenic properties of a de Novo transmembrane model peptide depend on the length of the hydrophobic core. *J. Biol. Chem.* **2007**, *282*, 18388–18396.
- (35) Melikyan, G. B.; Markosyan, R. M.; Roth, M. G.; Cohen, F. S. A point mutation in the transmembrane domain of the hemagglutinin of influenza virus stabilizes a hemifusion intermediate that can transit to fusion. *Mol. Biol. Cell* **2000**, *11*, 3765–3775.
- (36) Sternberg, M.; Ali, S. N.; Helmer-Citterich, M.; Gherardini, P. F.; Fleming, K.; Kelley, L. A.; Wass, M. N. Evolution of protein structure and function. *Comp. Biochem. Physiol., Part A: Mol. Integr. Physiol.* **2009**, *153A*, S47.
- (37) Holt, A.; Killian, J. A. Orientation and dynamics of transmembrane peptides: the power of simple models. *Eur. Biophys. J. Biophys. Lett.* **2010**, *39*, 609–621.
- (38) Yau, W. M.; Wimley, W. C.; Gawrisch, K.; White, S. H. The preference of tryptophan for membrane interfaces. *Biochemistry* **1998**, *37*, 14713–14718.
- (39) Armstrong, R. T.; Kushnir, A. S.; White, J. M. The transmembrane domain of influenza hemagglutinin exhibits a stringent length requirement to support the hemifusion to fusion transition. *J. Cell Biol.* **2000**, *151*, 425–437.
- (40) Armstrong, R. T.; Kushnir, A. S.; White, J. M. Length requirements of the influenza hemagglutinin transmembrane domain for membrane fusion: 17 amino acids yield full fusion, but 15 amino acids yield only hemifusion. *Mol. Biol. Cell* **1999**, *10*, 299A.
- (41) Neumann, S.; Langosch, D. Conserved conformational dynamics of membrane fusion protein transmembrane domains and flanking regions indicated by sequence statistics. *Proteins: Struct., Funct., Bioinf.* **2011**, *79*, 2418–2427.
- (42) Tatulian, S. A.; Hinterdorfer, P.; Baber, G.; Tamm, L. K. Influenza Hemagglutinin Assumes a Tilted Conformation during Membrane-Fusion as Determined by Attenuated Total-Reflection Ftir Spectroscopy. *EMBO J.* **1995**, *14*, S514–S523.
- (43) Killian, J. A.; dePlanque, M.; vanderWel, P.; Koeppe, R. E.; Greathouse, D. V. Induction of non-bilayer structures by alpha-helical peptides in a model membranes of diacylphosphatidylcholine and diacylphosphatidylethanolamine. *Biophys. J.* **1996**, *70*, Wp267.
- (44) van der Wel, P. C. A.; Pott, T.; Morein, S.; Greathouse, D. V.; Koeppe, R. E.; Killian, J. A. Tryptophan-anchored transmembrane peptides promote formation of nonlamellar phases in phosphatidylethanolamine model membranes in a mismatch-dependent manner. *Biochemistry* **2000**, *39*, 3124–3133.
- (45) Lee, M. T.; Hung, W. C.; Chen, F. Y.; Huang, H. W. Mechanism and kinetics of pore formation in membranes by water-soluble amphipathic peptides. *Proc. Natl. Acad. Sci. U. S. A.* **2008**, *105*, 5087–5092.
- (46) Strandberg, E.; Ozdirekcan, S.; Rijkers, D. T. S.; van der Wel, P. C. A.; Koeppe, R. E.; Liskamp, R. M. J.; Killian, J. A. Tilt angles of transmembrane model peptides in oriented and non-oriented lipid bilayers as determined by H-2 solid-state NMR. *Biophys. J.* **2004**, *86*, 3709–3721.
- (47) Thomson, J. D.; Higgins, D. G.; Gibson, T. J. CLUSTAL W: improving the sensitivity of progressive multiple sequence alignment through sequence weighting, positions-specific gap penalties and weight matrix choice. *Nucleic Acids Res.* **1994**, *22*, 4673–4680.
- (48) Harrison, S. C. Viral membrane fusion. *Nat. Struct. Mol. Biol.* **2008**, *15*, 690–698.
- (49) Martens, S.; McMahon, H. T. Mechanisms of membrane fusion: disparate players and common principles. *Nat. Rev. Mol. Cell Biol.* **2008**, *9*, 543–556.
- (50) White, J. M.; Delos, S. E.; Brecher, M.; Schornberg, K. Structures and mechanisms of viral membrane fusion proteins:



Multiple variations on a common theme. *Crit. Rev. Biochem. Mol. Biol.* **2008**, *43*, 189–219.

(51) Kordyukova, L. V.; Serebryakova, M. V.; Polyansky, A. A.; Kropotkina, E. A.; Alexeevski, A. V.; Veit, M.; Efremov, R. G.; Filippova, I. Y.; Baratova, L. A. Linker and/or transmembrane regions of influenza A/Group-1, A/Group-2, and type B virus hemagglutinins are packed differently within trimers. *Biochim. Biophys. Acta, Biomembr.* **2011**, *1808*, 1843–1854.